[16] E. M. T. Jones, "Wide-band strip-line magic-*T*," *IRE Trans. on Microwave Theory and Techniques*, vol. MTT-8, pp. 160–168, March 1960.
[17] D. I. Kraker, "Asymmetric coupled-transmission-line magic-*T*," *IEEE Trans. on Microwave Theory and Techniques*, vol. MTT-12, pp. 595–599, November 1964.
[18] K. Itakura, S. Yamamoto, and T. Azakami, "Coupled strip-line hybrid circuit" (in Japanese), presented at the 1966 Joint Meeting of the Four Electrical Institutes of Japan, no. 1069.
[19] S. B. Cohn, "Characteristic impedances of broadside-coupled strip transmission lines," *IRE Trans. on Microwave Theory and Techniques*, vol. MTT-8, pp. 633–637, November 1960.
[20] T. Ikeda and R. Sato, "Characteristic impedances of broadside-coupled strips parallel to the ground planes" (in Japanese), presented at the 1965 Joint Meeting of the Four Electrical Institutes of Japan, no. 1459.
[21] W. J. Getsinger, "A coupled strip-line configuration using printed-circuit construction that allows very close coupling," *IRE Trans. on Microwave Theory and Techniques*, vol. MTT-9, pp. 535–544, November 1961.
[22] J. P. Shelton, "Impedances of offset parallel-coupled strip transmission lines," *IEEE Trans. on Microwave Theory and Techniques*, vol. MTT-14, pp. 7–15, January 1966.
[23] T. Arakawa, "Edge effect correcting method" (in Japanese), *Reports of University of Electro-Communications, Tokyo*, no. 5, December 1953.
[24] S. B. Cohn, "Thickness corrections for capacitive obstacles and strip conductors," *IRE Trans. on Microwave Theory and Techniques*, vol. MTT-8, pp. 638–644, November 1960.
[25] G. W. Spenceley and R. M. Spenceley, *Smithsonian Elliptic Functions Tables*, Smithsonian Miscellaneous Collections, vol. 109, Washington, D.C.: Smithsonian Institute, 1947.
[26] F. Oberhettinger and W. Magnus, *Anwendung der Elliptischen Funktionen in Physik und Technik*. Berlin: Springer-Verlag, 1949.
[27] L. M. Milne-Thomson, *Die Elliptischen Funktionen von Jacobi*. New York: Dover, 1950, Tables (reprint).
[28] H. Nagaoka and S. Sakurai, "Tables of theta functions, elliptic integrals *K* and *E*, and associated coefficients in the numerical calculation of elliptic functions," Table 1, vol. II, *Scientific Papers of the Institute of Physical and Chemical Research*, Tokyo, Japan, 1922.
[29] S. Tomochika, *Elliptic Functions* (in Japanese). Tokyo: Kyoritsu, 1958.

Some Designs of X_L-Band Diode Switches

R. N. ASSALY

Abstract—**X_L-band waveguide switches, using PIN diodes for the switching elements, were developed in the SPST, SP2T, SP4T, and SP8T configurations. At the frequency of 7.75 GHz, for which they were tuned, they exhibited insertion losses on the average of 0.1, 0.4, 0.6, and 1.1 dB, respectively. In all cases, the signal going out of each switch port when turned OFF decreased in excess of 29 dB. The bandwidth of each switch, whose values are indicated, is narrower for the switch which has the larger number of ports or which contains diodes of lower capacitance. Semiempirical formulas are developed which predict performance characteristics of the SPST switch in particular.**

I. Introduction

MICROWAVE SWITCHES, which are operated by the action of diodes, are used increasingly in microwave systems because of their valuable advantages of light weight and low driving (or bias) power. In the X-band region, only SPST switches are reported in the literature [1]–[10] (to this writer's knowledge) and a few SP2T and (special-order) SP4T switches are available commercially [11]. The limitations encountered in the design of the multithrow switch are primarily due to RF losses. The switch, in essence, consists of a number of SPST units mounted in a transmission line junction, and its loss is the combined loss of all the SPST units as well as the junction. Those SPST switches that were reported had insertion losses in the ON state in excess of 1/2 dB and generally about 1 dB. In the OFF state, insertion losses ranged as low as 20 dB (which also represents a loss in the multithrow switch). Some high insertion losses have been achieved but at the expense of bandwidth or high insertion loss in the ON state. To design a multithrow switch with good characteristics is contingent upon the development of an SPST unit with correspondingly better characteristics in both the ON and OFF states.

The switches in this paper were developed for a specific application where they had to give their best performance at 7.75 GHz in the X_L-band region and had to have a broad bandwidth. However, this should not limit their usefulness, for the principles set forth are applicable in general.

The SPST switch will be described first, followed by the SP4T, the SP2T, and the SP8T switch. Before the switches could be developed in detail, however, it was necessary to make educated guesses as to which basic designs would produce the best characteristics, as will be outlined in the following section. The descriptions in this paper are for the small-signal application. Measurements to determine the dependence of a switch characteristic on the RF power level or the power limitations will not be reported.

Manuscript received March 1, 1966; revised August 2, 1966.
The author is with the M. I. T. Lincoln Laboratory, Lexington, Mass. (Operated with support from the U. S. Air Force.)

II. Preliminary Considerations

The initial activity was to design an SPST switch, a two-port device in which the power would be reflected with minimum loss in the OFF state, and would pass through with minimum loss in the ON state. This is equivalent to an impedance shunting a transmission line that changes from one of very low magnitude to one of very high magnitude. Next, n of these switches were to be incorporated in an $(n+1)$-port device which would constitute an SPnT switch. The one port not containing a SPST switch would be the input. One switch would be ON, and the other $(n-1)$ switches would be OFF.

A diode can be represented by an impedance with resistive and reactive components. Their values change with bias, and for the two biases that shall be used, the impedance shall be ascribed values R_r+jX_r and R_f+jX_f. For low power loss, the values of the R's must be small, and at this point shall be assumed small. If we add a series reactive component

$$X_s = -X_r, \tag{1}$$

at one bias the total impedance is R_f. Its value is low and thus can be used for the OFF state. For the other bias, the impedance is $R_f+j(X_f-X_r)$. If we add a parallel reactance

$$X_p = -(X_f - X_r), \tag{2}$$

the net impedance is high and can thus be used for the ON state. If the total network is placed across a transmission line of characteristic impedance Z_0, we obtain finally the circuit of Fig. 1. The box labeled "diode" would represent not only the diode crystal itself but also the reactance of the diode leads and any structure supporting it. The elements external to it are devices added purposely to obtain the desired impedances.

In the OFF state, the input impedance is given by

$$\frac{1}{Z_{Lr}} = \frac{1}{R_r} - \frac{1}{j(X_f - X_r)} + \frac{1}{Z_0}. \tag{3}$$

For small R_r,

$$Z_{Lr} \simeq R_r \tag{4}$$

and the standing-wave ratio is approximately

$$r \approx \frac{Z_0}{R_r}. \tag{5}$$

In the ON state, the input impedance is given by

$$\frac{1}{Z_{Lf}} = \frac{1}{R_f + j(X_f - X_r)} - \frac{1}{j(X_f - X_r)} + \frac{1}{Z_0}. \tag{6}$$

For small R_f,

$$\frac{1}{Z_{Lf}} \simeq \frac{R_f}{(X_f - X_r)^2} + \frac{1}{Z_0}, \tag{7}$$

and the insertion loss, the ratio of the power propagating past the network to the power incident on it, is given approximately by

$$IL_f \simeq \frac{1}{\left[1 + \dfrac{R_f Z_0}{2(X_f - X_r)^2}\right]^2}. \tag{8}$$

Next the networks are combined with a junction to produce the circuit of Fig. 2. If the networks are placed an odd number of quarter wavelengths from the junction, the impedance of Z_{Lr} is Z_0^2/R_r at the junction. There are $(n-1)$ of them in parallel, and the insertion loss due to them is

$$IL' \simeq \frac{1}{\left[1 + (n-1)\dfrac{R_r}{2Z_0}\right]^2}. \tag{9}$$

Multiplying with the value of IL at the second impedance Z_{Lf}, (8), the total loss is given by

$$IL_T \simeq \frac{1}{\left\{\left[1+(n-1)\dfrac{R_r}{2Z_0}\right]\left[1+\dfrac{R_f Z_0}{2(X_f-X_r)^2}\right]\right\}^2}. \tag{10}$$

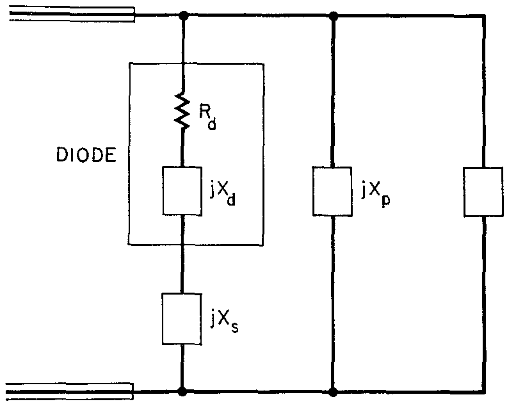

Fig. 1. The diode network across a transmission line. In the OFF state, $R_d=R_r$ and $X_d=X_r$. In the ON state, $R_d=R_f$ and $X_d=X_f$.

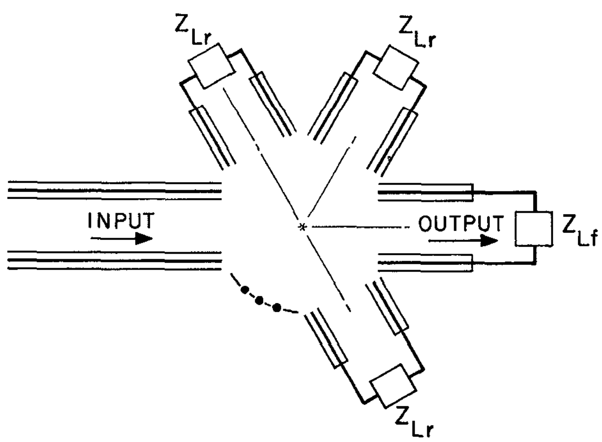

Fig. 2. The SPnT switch utilizing an idealized junction. The diode networks are an odd number of quarter wavelengths from the junction.

It should be noted that this result shows that the loss in the SPnT switch depends only on the insertion loss of the SPST switch in the ON state and on its standing-wave ratio in the OFF state.

The ideal value of IL_T is one (that is, there is no power loss). To approach this, R_r and R_f should be small and $|X_f - X_r|$ should be large. The remaining parameter Z_0 has an optimum that is found by differentiating (10). The approximate solution is

$$Z_0 \simeq |X_f - X_r| \sqrt{(n-1)\frac{R_r}{R_f}}. \tag{11}$$

If (11) is substituted into (10), one obtains an optimum value for IL_T which depends only on the characteristics of the diode. Let us now consider the diode, specifically the PIN type, which exhibits better characteristics than other types for this application.

On reverse or negative bias the diode draws very little power and because all but one diode in the switch is in the OFF state, reverse bias is chosen for these diodes and the switches designed on this basis. The power then needed to operate a switch will be taken almost entirely by the single diode in the ON state where the bias is forward or positive. A second reason for this choice will be seen in the method of tuning described in Section III.

On reverse bias,

$$X_r \simeq \omega L - \frac{1}{\omega C} \tag{12}$$

where L consists of the inductances of the diode leads and C consists of the capacitances of the semiconductor junction and the diode case.

On forward bias,

$$X_f \simeq \omega L \tag{13}$$

since the capacitance is now shunted by a low resistance causing its effect to be negligible. Both resistances R_r and R_f may be of the order of 1 or 2 ohms at X-band.

The factor $|X_f - X_r|$ then has the value

$$|X_f - X_r| = \frac{1}{\omega C}. \tag{14}$$

Thus, to have a large value of $|X_f - X_r|$, we want a small value of C. At present, the value of C is limited to about 0.3 pF. The diodes used in the switches described later had values of C ranging from 0.30 to 0.46 pF. At $f = 7.75$ GHz, the corresponding value of $|X_f - X_r|$ is 70 to 50Ω. If we assume values of 60Ω for $|X_f - X_r|$ and 1.5Ω for both R_r and R_f, values found for the total loss for different impedances Z_0 using (10) are given in Table I in three sets. The first set is for the optimum value of Z_0, given by (11). The second set is the loss for $Z_0 = 60\Omega$, and the third set is for $Z_0 = 360\Omega$, the $V-I$ characteristic impedance of standard WR-112 waveguide at $f = 7.75$ GHz. As will be seen from the experimental data, these values are somewhat optimistic.

TABLE I
THEORETICAL LOSSES OF THE SPnT SWITCH FOR VARIOUS VALUES OF CHARACTERISTIC IMPEDANCE Z_0

n	Z_0 (ohms)	Insertion Loss (dB)	Z_0 (ohms)	Insertion Loss (dB)	Z_0 (ohms)	Insertion Loss (dB)
2	60	0.22	60	0.22	360	0.65
4	104	0.37	60	0.43	360	0.68
8	159	0.57	60	0.84	360	0.75

Some attention shall now be given to the bandwidth. In altering the frequency, the relevant parameters that change are the reflection coefficients at each OFF diode network, the insertion loss of the ON diode, and the separation in wavelengths of the diodes from the junction. Without actually determining the total effect of these changes, it is more pertinent to ask what can be done to minimize each of them. For this aspect of the problem, resistances shall be neglected. Also the conditions expressed in (1) and (2) shall now be taken to hold at one specific frequency $\omega = \omega_0$.

Referring to Fig. 1, the reflection coefficient can be found:

$$\Gamma = -\frac{1}{1 + j\Omega_r}, \tag{15}$$

where

$$\Omega_r = \frac{2}{Z_0} \frac{(X_r + X_s)X_p}{X_r + X_s + X_p}. \tag{16}$$

The change of Γ from the ideal value of 1 with the change of frequency from resonance can be inferred from the differential

$$\left.\frac{d\Omega_r}{d\omega}\right|_{\omega=\omega_0}.$$

By differentiating (16) and substituting (1) and (12), we get

$$\left.\frac{d\Omega_r}{d\omega}\right|_{\omega=\omega_0} = \frac{2}{Z_0}\left(L + \frac{1}{\omega_0^2 C} + \left.\frac{dX_s}{d\omega}\right|_{\omega=\omega_0}\right). \tag{17}$$

All the terms of this equation are positive ($dX_s/d\omega$ cannot be negative, a result of Foster's reactance theorem for a lossless network). Hence, each term must be small if Ω_r is to stay small with a frequency change. Or we want a small L, a large C, a small $dX_s/d\omega$, and a large Z_0. As we saw earlier, the higher C gives the higher switch loss. The choice of C must depend on the relative importance of loss and bandwidth. The magnitude of $dX_s/d\omega$ depends, of course, on the hardware, but it may be noted that if the diode is nearly self-resonant, then X_s and $dX_s/d\omega$ can be made small.

For the diode in the ON state, the insertion loss is

$$IL_f = \frac{1}{1 + \Omega_f^2}, \tag{18}$$

where

$$\Omega_f = \frac{Z_0}{2} \frac{X_f + X_s + X_p}{(X_f + X_s)X_p}. \qquad (19)$$

Just as before, the net change of IL_f from the ideal value of one with the change of frequency from resonance can be inferred from the differential

$$\left.\frac{d\Omega_f}{d\omega}\right|_{\omega=\omega_0}.$$

By evaluating this and substituting (1), (2), (12), and (13), the results indicate that C and $dX_p/d\omega$ should be small. However, as we shall see later, this diode has considerably less effect on narrowing the bandwidth than do the diodes on reverse bias.

If the diode networks are placed a distance s from the switch junction, s should also be small, but should be nominally an odd number of quarter wavelengths. Also the transmission line cutoff frequency should be minimized.

Considering all the parameters that change with frequency, the effect of most of them is to give rise to signal reflections, which in part propagate back through the input port of the switch as well as alter the signals in the OFF ports. One may suppose that with an appropriate switch design, they can be matched and, in this sense, the energy is not lost. This is not the case for the diodes in the OFF state. There, the fraction of the energy that is not reflected, as implied in (15), is truly lost and therefore the major concern is the terms of the equation.

Having estimated the characteristics of a switch, reasonable choices could be made for the diode and the transmission line type. The PIN diode has several advantages over other kinds.

1) Its characteristics are quite insensitive to bias over a large positive or negative range of bias. In the small range about zero bias, the series resistance and reactance do vary rapidly with change in bias.
2) The series resistance in both states is lower than for other types of diodes presently available.
3) It exhibits a larger $|X_f - X_r|$ value.

PIN diodes with lower R and higher $|X_f - X_r|$ (that is, lower C) are available in a standard package, hermetically sealed, and consisting of a ceramic body bonded to gold-plated metal lugs. This body is 0.062 inch long by 0.080 inch in diameter.

For the transmission line, a waveguide is preferable to a coaxial line or a strip line for at least two reasons—its losses are less, and a diode shunting the waveguide will have both its terminal lugs relatively more accessible. In choosing the waveguide, its walls must be spaced roughly the length of the diode body or the diode must be supported at the end of the post. This second choice is undesirable because of the inductance introduced by the post, with due respect to the results inferred from (17). Furthermore, the impedance of a narrow-height waveguide is nearer the optimum value given by (11).

Lastly, we would like to reduce the cutoff frequency. There are two ways to do this—the wide dimension of the waveguide may be increased, or a ridge guide may be used. The second alternative gives a little more freedom in the choice of impedance and cutoff wavelength if the separation of the waveguide walls at its centerline is restricted.

III. The SPST Switch

A. Description and Performance

The SPST switches that were constructed and tested have the cross section shown in Fig. 3. The transmission line chosen is a ridge guide with inside dimensions 1.122 by 0.125 inches, where the ridge is 0.378 by 0.051 inche. The gap at the center of the guide is about the same as the length of the diode body. The 0.378-inch dimension was chosen to give close to the lowest value of cutoff frequency, the other dimensions being fixed. Based on the equations given in the article by S. Hopfer [12], the guide wavelength at 7.75 GHz is 1.847 inches. The V-I characteristic impedance, based on the article by T. G. Mihran [13], is found to be 56.3 Ω at 7.75 GHz, which is near the desired optimum. Again from Hopfer, the attenuation is found to be 0.41 dB/m for an aluminum guide.

To provide the series reactance X_s, a coaxial transmission line is used which is shorted at one end, and whose center conductor supports the diode at the other end. The reactance X_s is then the reactance of the coaxial line at the diode:

$$X_s = Z_{0c} \tan \frac{\omega l}{c}, \qquad (20)$$

where l is its length, and Z_{0c} is its characteristic impedance (which is 31.4 Ω for this geometry). If $dX_s/d\omega$ is to be small, in accordance with the bandwidth considerations, length l must be small. The reactance X_s must then be small, and furthermore must be positive. Then for resonance in the OFF state, the diode reactance X_r must be negative. Since this is possible only for reverse bias, the second reason for designing the switches to have the OFF diodes on reverse bias is established. It is also apparent that there is an upper limit on the diode capacitance, since if it is too large, the total reactance of the diode becomes positive. Restating all this, for a broader bandwidth, the diode should have a self-resonance at a frequency above the design frequency but near it.

To allow for variations in diode characteristics, the coaxial line must be variable in length. This is made possible by a 00-96 screw that travels up and down the channel between the inner and outer conductors and shorts one to the other. The end of the screw effectively defines the position of the shorted end of the coaxial line.

To provide the parallel resonance on forward bias, reactance X_p must be negative. This is obtained by a capacitive iris located in the waveguide at the plane of the diode. The gap between the iris and waveguide wall was adjusted to produce the best match at 7.75 GHz using the same diode with which the detailed measurements described below were made. It was found that the iris need not be adjustable, that it was unnecessary to make it tunable for there is not sufficient variation in characteristics from one piece to the next.

One more notable item is the coupling-RF choke arrangement used. It couples the bias to the diodes and keeps the RF leakage at a sufficiently low level that the increase in the losses is negligible. It consists of two radial transmission lines in series, each nominally a quarter wavelength long. The first radial line has a very low characteristic impedance because of the small spacing between conducting surfaces, and the second has an impedance an order of magnitude larger. Rough measurement of the leakage showed it to be at least 50 dB down from the power flowing to the switch.

Figure 4 shows the switch with the diode and capacitive iris visible.

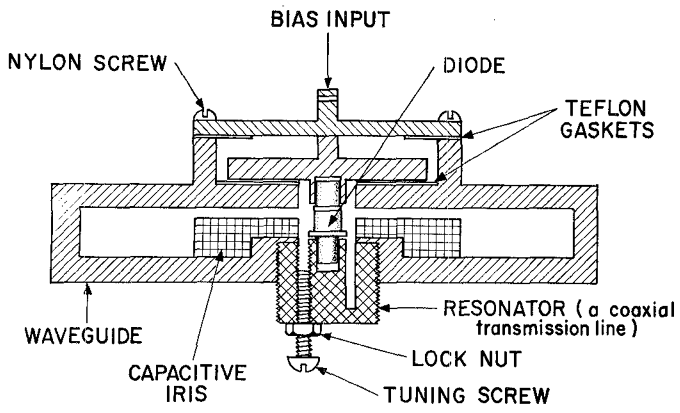

Fig. 3. Cross section of the SPST switch at the diode.

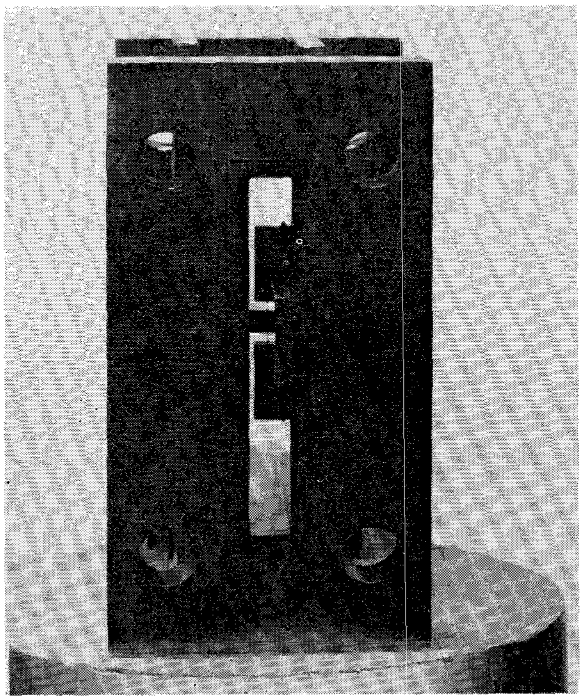

Fig. 4. Looking inside the SPST switch.

Figure 5 presents graphs of the measured characteristics of such a switch using a PIN diode obtained from a manufacturer who quoted the characteristics: total capacitance at -50 V, 1 MHz→0.34 pF, series resistance at $+100$ mA, 500 MHz→1.08Ω.

(For all switch measurements given in this report, the biases are -70 V for reverse bias and $+35$ mA for forward bias. Preceding the measurements of a switch, the 00-96 screw at each diode is adjusted so as to minimize the signal propagating past the diode in the OFF state. In all cases, this adjustment is made at 7.75 GHz. This procedure will henceforth be referred to as "tuning the diode.")

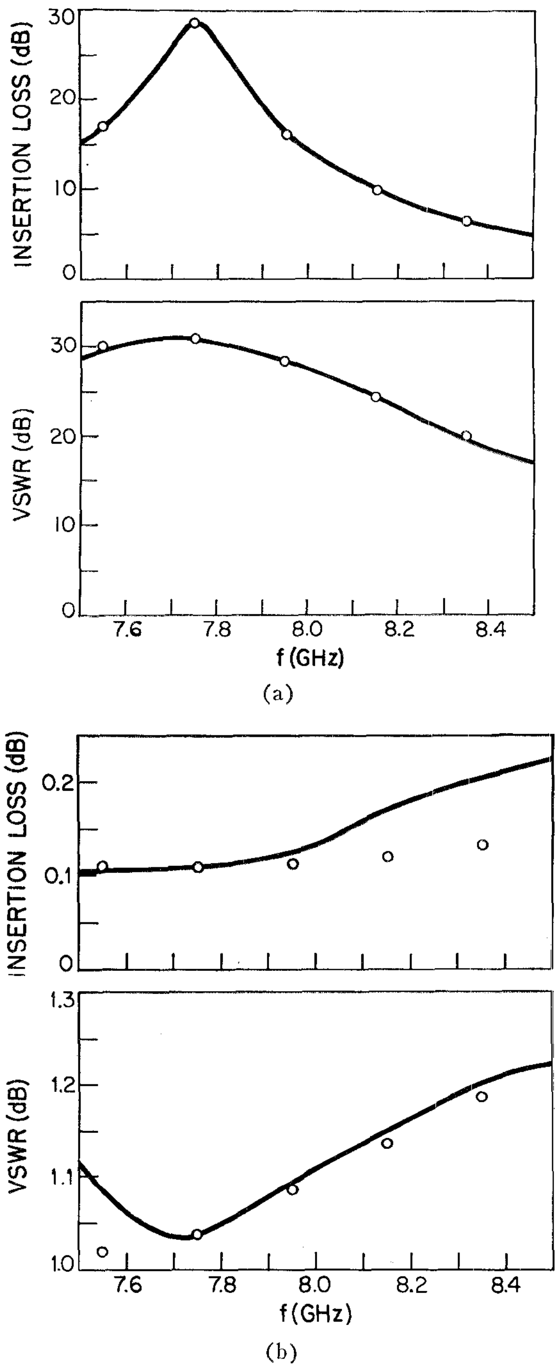

Fig. 5. Measured characteristics of an SPST switch, where the circled points indicate values calculated on the basis of the semi-empirical theory described in the text. (Diode characteristics: 0.34 pF, 1.08 Ω. See text.) (a) Reverse bias. (b) Forward bias.

B. Relating Experiment to Theory

It is of interest to check the measurements with theory. Or more practically, it is useful to have a set of equations that predict the performance of a switch for different diode characteristics. Also, an application of this theory is that it can be employed in attempts to predict the behavior of the SPnT switch by combining the SPST characteristics with those of the switch junction.

In terms of the parameters of the network shown in Fig. 1, and without any approximations,

$$\Gamma = \left[\frac{(1-bx)^2+(b\rho)^2}{x^2+\rho^2+(1-bx)^2+(b\rho)^2+2\rho}\right]^{1/2} \cdot \exp j\left(\tan^{-1}\frac{b\rho}{1-bx} - \tan^{-1}\frac{b\rho+x}{1-bx+\rho}+\pi\right) \quad (21)$$

and

$$IL = \frac{x^2+\rho^2}{x^2+\rho^2+(1-bx)^2+(b\rho)^2+2\rho}, \quad (22)$$

where

$$x = 2\frac{X_d+X_s}{Z_0}, \quad (23)$$

$$\rho = 2\frac{R_d}{Z_0}, \quad (24)$$

$$b = -\frac{Z_0}{2X_p}, \quad (25)$$

and the reactance X_d is given by (12) or (13). These equations are applicable for either bias, and appropriate subscripts r or f will be added when referring to one bias only.

The condition for resonance, reverse bias, is now

$$x = x_{r0} = 0. \quad (26)$$

Equations (21) and (22) reduce to

$$|\Gamma_{r0}|^2 = \frac{1+(b\rho_r)^2}{(1+\rho_r)^2+(b\rho_r)^2} \quad (27)$$

and

$$IL_{r0} = \frac{\rho_r^2}{(1+\rho_r)^2+(b\rho_r)^2}. \quad (28)$$

The resonant condition for forward bias, if satisfied, would be

$$x = x_{f0} = \frac{1}{b}. \quad (29)$$

The reactance X_p is prespecified but x_{f0} can have different values depending on the diode and hence (29) does not necessarily hold.

There is not enough information about the various parameters involved to check the experimental results with the equations above. On the other hand, it is impossible to choose parameters that fit the experimental results to the equations in all respects. However, by suitable manipulation, it was possible to get some correspondence. With this success, it was found that one could predict some of the performance of this type of switch for any diode using the value of capacitance quoted by the manufacturer. This will now be put forth in detail with respect to the characteristics plotted in Fig. 5.

The theoretical values of Z_0, Z_{0c}, and X_s were used in this analysis. It turned out to be somewhat more difficult to determine the value of the reactance X_p as well as its dependence on the frequency. Initially, values were found by measuring the standing-wave ratio of the switch with the diode absent, the assumption being that only the capacitive iris would be seen by the RF signal. From this measurement, the value derived for b was 0.44, remaining approximately constant over the frequency range. At first, this value was used in the reverse bias analysis. Then going to the forward bias case, the calculated VSWR uniformly increased from 1.14 at 7.55 GHz to 1.28 at 8.45 GHz, indicating only fair agreement. By choosing X_p to have a form

$$X_p = -\frac{1}{\omega C_p}, \quad (30)$$

where $C_p = 0.28$ pF, good agreement was then found in the forward bias case and proved to have little effect on the analysis for the reverse bias case.

At resonance, for reverse bias, the insertion loss measured 28.6 dB. By (28), the value of ρ_r is then 0.039. Equation (27) indicates that $|\Gamma_{r0}|$ should then have the value 0.96 and hence the standing-wave ratio $r_{r0} = 34.4$ dB. However, r_{r0} measured 31.0 dB. To justify this discrepancy, it was assumed that there were line losses between the diode and the point of measurement of the standing-wave ratio. Then, if this loss amounts to 0.08 dB and with $R_r = 1.09\ \Omega$, (27) and (28) give values in agreement with the experiment.

Let us now consider what happens at a frequency not at resonance, say 8.35 GHz. At 8.35 GHz, the insertion loss measured 6.5 dB. Then, by (22), $x_r = 0.46$. Equations (23), (12), and (20) relate x to L, C, and ω. The values of x_r are now known for two values of ω, and hence the two simultaneous equations can be solved for L and C. The length l is needed and measures 4.0 mm. Hence, $L = 1.10$ nH, and $C = 0.265$ pF. The inductance is near the value, 0.9 nH, quoted by the manufacturer, and any difference can be accounted for in the structure supporting the diode. The capacitance is somewhat lower than the quoted value, 0.34 pF, for several possible reasons: 1) the frequency at which the manufacturer measured C is different, 2) the theory is too inaccurate, and/or 3) the capacitance is partly shielded by the walls of the waveguide. If the calculated values are accepted, the characteristics r_r and IL_r can be determined for any other frequency. The circled points in Fig. 5(a) are some of the values calculated from (21) and (22) taking into account the effect of the postulated line loss. The agreement is very good (understandably, because, in a sense, the curves were "fitted").

On forward bias at resonance, x_{f0} can be calculated from (23), (13), and (20) where all the parameters are now known. IL_{f0} measures 0.975 (0.11 dB); hence to satisfy (22) and (24), $R_f = 1.8\ \Omega$. Here it was assumed that there were no line losses. If the resistance is taken as 1.1 Ω, the value quoted by the manufacturer, a line loss of 0.036 dB is needed to account for the total loss. As it works out, it makes little difference which situation is assumed in calculating the insertion loss or VSWR at any frequency. The circled points in Fig. 5(b) are the calculated values using (21) and (22) and the form of X_p given in (30).

We have now reached a point where we would have to know the dependence of the characteristics on the diode capacitance. By tests with other diodes, it was found that if 0.075 pF were subtracted from the value quoted by the manufacturer and the value $L = 1.10$ nH used in all cases, the experiments agreed fairly well with the theory. It is necessary in each case that l be chosen so that (26) is satisfied. Figure 6 is a set of three plots based on (21) and (22) for three different quoted capacitances C'. The values of ρ and line losses were chosen to be the same as in the case investigated. The largest capacitance, 0.46 pF, corresponds to $l = 0$. The diode capacitance is bound to this limit if the bandwidth is to be kept large. The smallest value, 0.30 pF, is the limit set by the manufacturing process (at present). The main point about these curves is that the bandwidth is broader for the higher capacitance.

The tests that were carried out on other diodes on reverse bias gave results within -2 dB to $+\frac{1}{2}$ dB of the value calculated by (21) or (22). This indicates that the diode from which the parameters were derived performed better than the average for its quoted capacitance. There was no good correlation between the measured values and the resistance quoted by the manufacturer. The only conclusion that could be drawn was that if the quoted resistance is less than 1.2 Ω, the insertion loss will be lower than 0.2 dB on forward bias and the VSWR higher than 28 dB on reverse bias at resonance.

Another piece of useful information concerning the SPST switch is the phase of the reflection coefficient, the exponent in (21). It was found that if the reflection coefficient phase were measured and transferred to a plane 0.013 inch away from the plane at the center of the diode-reactance hardware in the direction of the generator, the experimental value agreed with the theoretical to within a degree over the frequency range. At 7.75 GHz, the phase is 180° and at 8.35 GHz, the phase is 154°.

Finally, one might ask at how high a frequency this switch may be tuned. For resonance on reverse bias, (26) holds; hence from (26), (23), (12), and (20) we have

$$\omega = \sqrt{\frac{1}{LC} + \left(\frac{Z_{0c}}{2L} \tan \frac{\omega l}{c}\right)^2} - \frac{Z_{0c}}{2L} \tan \frac{\omega l}{c} \cdot \qquad (31)$$

Theoretically, length l may be adjusted so that the tangent terms have a large negative value and apparently there is no limit on the value of ω. From the practical view, l would be large enough to increase the losses and narrow the bandwidth somewhat. If this is unacceptable and l is restricted to a small dimension, the maximum ω occurs at $l = 0$ for which

$$\omega = \omega_m = \frac{1}{\sqrt{LC}} \cdot \qquad (32)$$

For the diode of our experimental switch, $L = 1.10$ nH and $C = 0.265$ pF. Hence, the corresponding frequency is 9.32 GHz. By the same logic, if a switch is to be tuned to 9.32 GHz, a diode having a capacitance of 0.265 pF or less must be used.

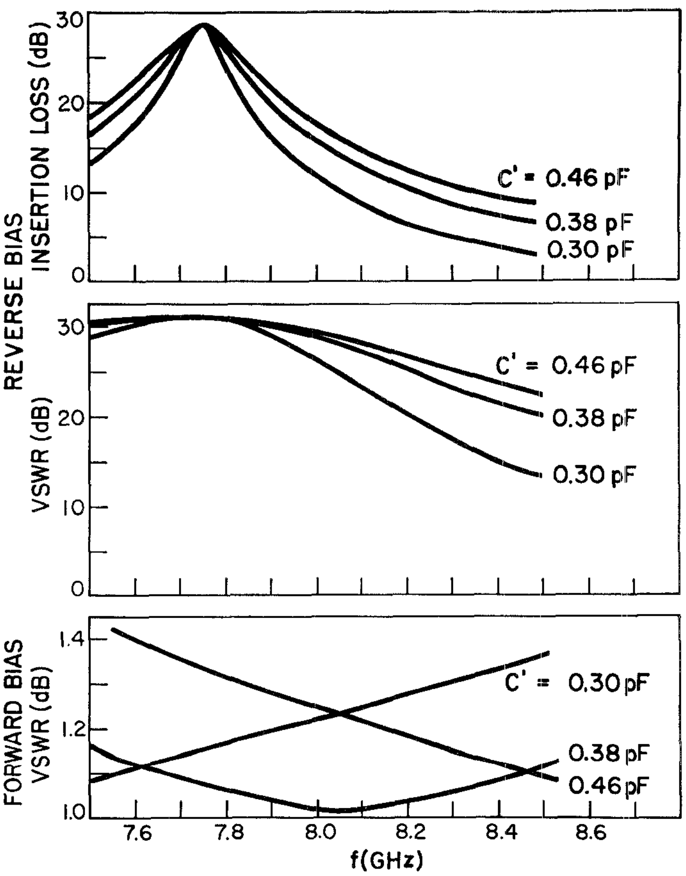

Fig. 6. Calculated characteristics of the SPST switch. It is assumed that the effective diode capacitance is 0.075 pF less than C', the value quoted by the manufacturer.

IV. The SP4T Switch

The designed SPST switch now had to be combined with a waveguide junction to yield the SP4T switch. This meant that such a junction had to be developed. The configuration chosen is shown in Fig. 7. The SPST units are contained in an H-plane cross having four-way symmetry. For our application, it was desired that the input be a waveguide so that to couple to the junction, a double waveguide-coaxial adapter was adopted into the design. All the waveguide ports are of the ridge geometry used in the SPST switch.

Because the SPST switch in the OFF state at resonance behaves nearly like a short circuit, the junction could be designed using movable shorts in three of the output ports. Provided that the shorts in the crosspiece be maintained at equal distances P from the coaxial center, four dimensions could be varied—the P dimension, the separation of the cross and the single guide, the distance from the short in the single guide to the coaxial center, and the diameter of the coaxial inner conductor. With these variables, it was possible to have the junction matched at 7.75 GHz. Moreover, the match could be controlled to a degree over a frequency band. But to have this sliding short circuit-junction combination broadband does not necessarily imply that the final switch will be broadband, because the SPST section does not behave like a short circuit in a fixed location as the frequency departs from 7.75 GHz. However, at this point, with no basis for choosing a bandwidth on which to adjust the junction-short combination, it was simply adjusted for a large value. One would feel intuitively at least that the standing waves existing in the switch are then less and the insertion loss correspondingly lower.

Once the values of the dimensions were established, an aluminum SP4T switch was built. In it, the SPST sections are situated so that at 7.75 GHz, the reflection from them in the OFF state would coincide in phase with the reflection from a short circuit if placed at distance P from the junction center. The output ports carry adapters to type OSM connectors whose VSWR values remain below 1.15 over the band from 7.7 to 8.4 GHz. Figure 8 illustrates a completed SP4T switch. Its weight is 210 grams.

Table II presents some of the characteristics measured for the switch at 7.75 GHz and at 8.35 GHz. The diode parameters are the values quoted by the manufacturer. The isolation is defined as the ratio of the signal propagating out of the ON port to the largest of the signals propagating out of the three OFF ports. Figure 9 gives plots of the insertion loss and isolation over a frequency range. Since all four ports differ in performance, average characteristics are given.

At frequencies away from 7.75 GHz, the signal level out of the OFF port physically opposite the ON port is higher than the other two OFF port signals. At 8.35 GHz, this difference amounts to about 2 dB. For this reason, one would expect the diode in this port to have a greater influence on the switch performance. In particular, the diode capacitance is the parameter in question as noted in Section III. Moreover, the ON port is broadband so as to exercise less influence. These points were checked from measurements made on a number of SP4T switches that were constructed and evaluated for our application. The diodes in them were chosen at random from a diode lot where the capacitances ranged from 0.30 to 0.46 pF. On each of these switches, the insertion loss and isolation for each port were measured. Figure 10 gives each isolation value vs. the capacitance of the diode in the port opposite the ON port, and the correlation of the two parameters can be seen.

Two other observations made on an SP4T switch at 7.75 GHz are worth mentioning. One is that RF power of up to 8 watts CW was passed through the switch with no apparent change in the insertion loss. The other is that it was found that the insertion loss increases with increasing temperature. At +100° C, the increase was about 0.2 dB. At −70° C, the insertion loss decreased by 0.35 dB.

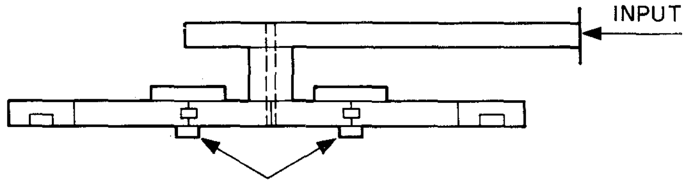

Fig. 7. Outline configuration of the SP4T switch.

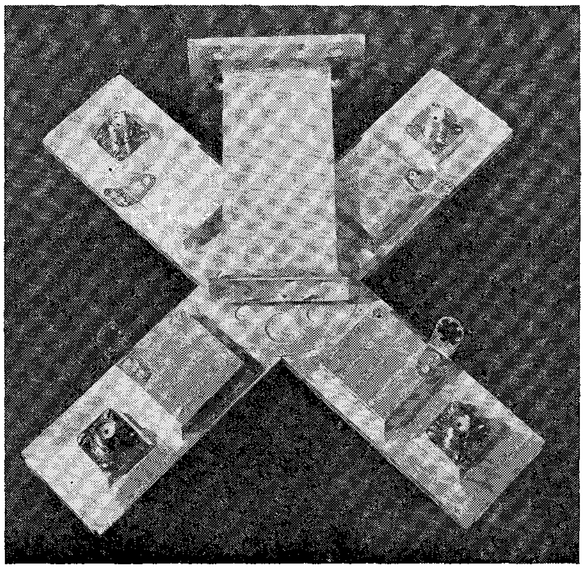

Fig. 8. The SP4T switch.

TABLE II
SOME MEASURED CHARACTERISTICS OF AN SP4T SWITCH

Port ON	ON Port Diode		f=7.75 GHz			f=8.35 GHz		
	C' (pF)	R (ohms)	VSWR	Insertion Loss (dB)	Isolation (dB)	VSWR	Insertion Loss (dB)	Isolation (dB)
1	0.45	0.79	1.06	0.63	29.5	2.0	4.4	8.1
2	0.45	1.27	1.04	0.66	31.3	2.1	4.6	7.7
3	0.45	0.70	1.10	0.58	28.4	2.1	4.2	9.6
4	0.44	0.97	1.21	0.65	30.0	2.1	4.4	8.4

The diode parameters are the values quoted by the manufacturer: C' is at -50 V, 1 MHz, and R is at $+100$ mA, 500 MHz. Isolation is defined here as the ratio of the signal propagating out of the ON port to the largest of the three signals propagating out of the OFF ports.

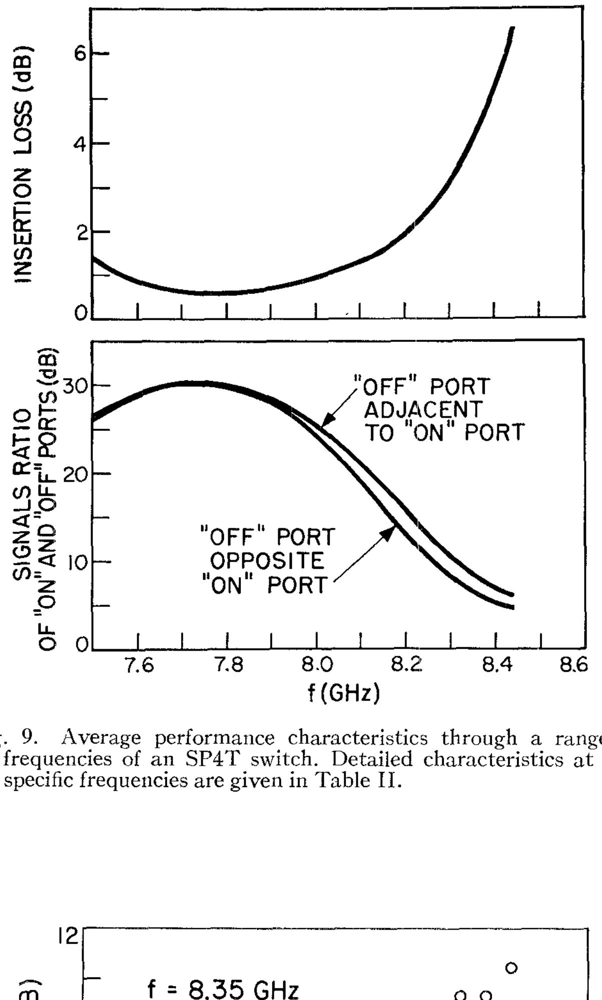

Fig. 9. Average performance characteristics through a range of frequencies of an SP4T switch. Detailed characteristics at two specific frequencies are given in Table II.

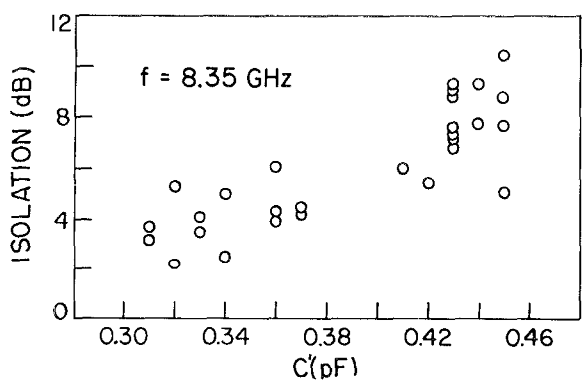

Fig. 10. Dependence of the SP4T switch isolation on diode capacitance. The circles are 28 experimental points for 7 switches where the values of C' refer to the diode in the port opposite the ON port.

V. THE SP2T SWITCH

An SP2T switch (Fig. 11) was designed, constructed, and tested. The output ports are similar to those of the SP4T switch. The input port is also similar in its method of operation in that the OFF diode acts like the shorting plate of the waveguide stub. The only requirement was that the diodes be situated the correct distance from the input.

The measured characteristics are summarized in Table III. Comparison of these results with those for the SP4T switch (Table II and Fig. 10) shows the SP2T switch to be better in performance. This is reasonable because it has fewer ports to leak power, and the junction arms are shorter implying a broader band.

Six SP2T switches were constructed and evaluated. Figure 12 gives each value of isolation measured vs. the capacitance of the diode in the OFF port at 8.35 GHz.

VI. THE SP8T SWITCH

It seemed reasonable that an SP8T switch could be constructed by mating two SP4T switches, such as the ones described in Section IV, where only one of the total of eight diodes would be ON for its operation. The logical way to put the SP4T switches together is shown in Fig. 13. Each SP4T section is fed by a coaxial line and the two coaxial lines join to the opposite sides of a WR-112 waveguide in which the RF signal enters. There were four dimensions to establish. As Fig. 13 shows, they are the separation P' of the diodes from the switch center line, the separation H of the SP4T sections from the WR-112 guide, the stub length Q of the WR-112 guide, and the inner conductor diameter d.

In a working switch, one of the SP4T sections contains the port that is ON. If this section can be matched to the coaxial line, it simplifies the switch design by reducing it to a development of two hardware pieces that individually are matched: a coaxial - SP4T section adapter, and a double coaxial - WR-112 adapter. The SP4T section whose ports are all OFF appears nearly like a short circuit whose location is important to the performance of the double coaxial - WR-112 adapter. The design of the double coaxial - WR-112 adapter can then be derived by using a matched load in one coaxial line to simulate one SP4T section and a short circuit in the other coaxial line to simulate the other.

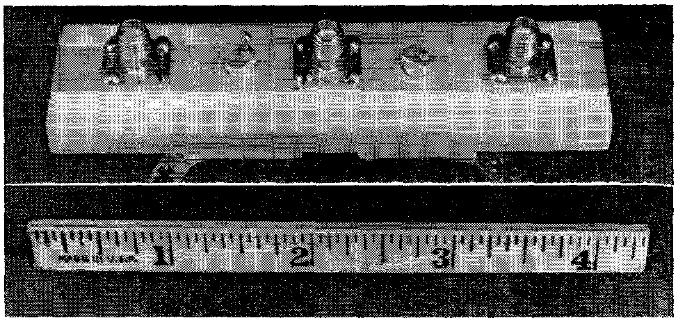

Fig. 11. The SP2T switch.

TABLE III

SOME MEASURED CHARACTERISTICS OF AN SP2T SWITCH

Port ON	ON Port Diode		$f=7.75$ GHz			$f=8.35$ GHz		
	C' (pF)	R (ohms)	VSWR	Insertion Loss (dB)	Isolation (dB)	VSWR	Insertion Loss (dB)	Isolation (dB)
1	0.37	1.08	1.25	0.35	32.3	1.43	1.23	7.8
2	0.35	0.79	1.24	0.31	32.0	1.41	1.10	8.7

The diode parameters are the values quoted by the manufacturer: C' is at -50 V, 1 MHz, and R is at $+100$ mA, 500 MHz. Isolation is defined here as the ratio of the signal propagating out of the ON port to that propagating out of the OFF port.

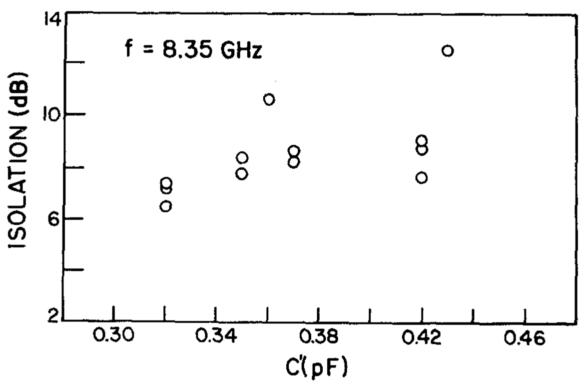

Fig. 12. Dependence of the SP2T switch isolation on diode capacitance. The circles are 12 experimental points for 6 switches where the values of C' refer to the diode in the OFF port.

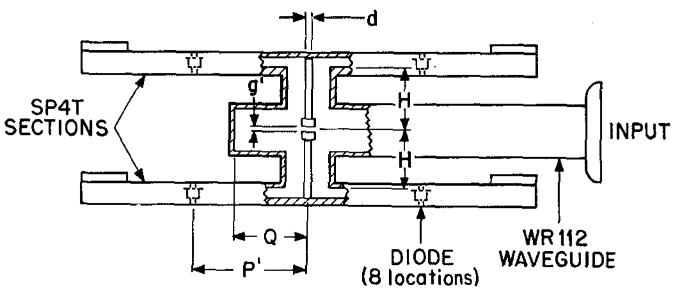

Fig. 13. Outline of the SP8T switch. One diode is ON, the other seven are OFF.

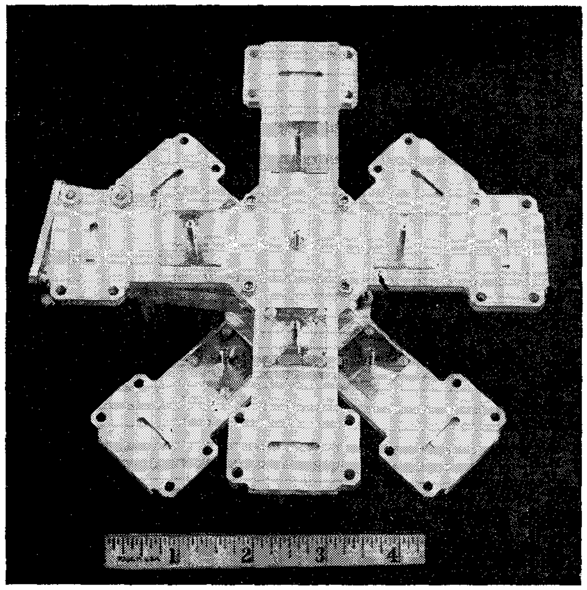

Fig. 14. The SP8T switch.

TABLE IV

SOME MEASURED CHARACTERISTICS OF AN SP8T SWITCH

Port ON	ON Port Diode		$f=7.75$ GHz		
	C'(pF)	R(ohms)	VSWR	Insertion Loss (dB)	Isolation (dB)
1	0.32	1.27	1.08	1.02	33.3
2	0.31	1.27	1.10	0.97	33.2
3	0.35	1.01	1.17	1.08	32.6
4	0.36	1.12	1.19	1.13	31.5
5	0.31	1.27	1.19	1.18	31.3
6	0.34	1.08	1.21	1.11	31.2
7	0.36	1.08	1.15	1.06	31.6
8	0.32	1.12	1.18	1.16	31.0

Ports 1 through 4 are on one SP4T section and ports 5 through 8 on the other. Column headings are as defined in Table II.

Once all the dimensions were established, an SP8T switch was constructed. As shown in Fig. 14, each port carries an adapter to mate to WR-112 waveguide. The adjustment of the switch calls for tuning the eight diodes and adjusting the two inner conductors (that is, the gap g) to minimize the highest VSWR of the eight values obtained with the eight ports ON in turn. The characteristics of the switch are summarized in Table IV. Measurements were made only at one frequency, 7.75 GHz.

VII. Conclusions

Switches were developed in the SPST, SP2T, SP4T, and SP8T configurations which all have good characteristics at a single frequency in the X-band region considering the present state of the art for these types of components. Some of their measured characteristics are indicated in Figs. 5, 9, and 10, and in Tables II, III, and IV. A semiempirical theory was developed for the SPST switch which could predict its performance in detail.

There are several points to note concerning these switch designs. First, the bandwidth of a switch, other than its dependence on the capacitances of the diodes, is narrower the larger the number of ports. A prime goal in further work should be to design switches with broader bandwidths in order to increase their usefulness. Second, use of a narrow-height rectangular waveguide rather than ridge guide would considerably simplify the fabrication of the switches. Also, adapters to waveguide of standard dimensions could easily be designed by well-developed procedures. Third, it may be possible to eliminate the iris that shunts each diode. By the theory pertaining to bandwidth in Section II, this would increase the bandwidth. There will be a large reflection of signal at the ON diode, but this should be possible to compensate by a matching network in the input port or by repositioning the diodes—the latter being more desirable.

On the surface, it is not clear what the combination of these various changes does to the overall performance, but at this date, a program is under way to find a switch design exhibiting these features and having a broad bandwidth. If it is successful, the results shall be reported at a later time.

Acknowledgment

The author wishes to acknowledge the guidance provided by L. J. Ricardi in this project. He also wishes to thank those involved in the mechanical design and fabrication of the components.

References

[1] D. Leenov, "PIN diode microwave switches and modulators," *Solid State Design*, vol. 6, pp. 37–40, April 1965; pp. 33–37, May 1965.

[2] R. V. Garver, et al., "Microwave semiconductor switching techniques," *IRE Trans. on Microwave Theory and Techniques*, vol. MTT-6, pp. 378–383, October 1958.

[3] T. H. B. Baker, "Semiconductor-diode waveguide switch," *Electronic Tech.*, vol. 38, pp. 300–304, August 1961.

[4] M. Bloom, "Microwave switching with computer diodes," *Electronics*, vol. 33, pp. 85–87, January 15, 1960.

[5] D. W. Feldman, and B. R. McAvoy, "A 100-db microwave semiconductor switch," *Rev. Sci. Instr.*, vol. 32, pp. 74–76, January 1961.

[6] V. J. Higgins, "X-band semiconductor switching and limiting using waveguide series tees," *Microwave J.*, vol. 6, pp. 77–82, November 1963.

[7] H. J. Peppiatt, et al., "A 7-Gc/s narrow-band waveguide switch using p-i-n junction diodes," *IEEE Trans. on Microwave Theory and Techniques*, vol. MTT-13, pp. 44–47, January 1965.

[8] H. S. Jones, Jr., and R. V. Garver, "Step-twist diode switch," *IEEE Trans. on Microwave Theory and Techniques* (*Correspondence*), vol. MTT-12, p. 549, September 1964.

[9] V. J. Higgins, "Semiconductor switching and limiting using 3-db short-slot (hybrid) couplers," *IEEE Trans. on Microwave Theory and Techniques* (*Correspondence*), vol. MTT-12, pp. 258–259, March, 1964.

[10] J. K. Hunton, and A. G. Ryals, "Microwave variable attenuators and modulators using *PIN* diodes," *IRE Trans. on Microwave Theory and Techniques*, vol. MTT-10, pp. 262–273, July 1962.

[11] A. Serchuk, "Solid-state switches," *Microwaves*, vol. 1, pp. 48–53, November 1962.

[12] S. Hopfer, "The design of ridged waveguides," *IRE Trans. on Microwave Theory and Techniques*, vol. MTT-3, pp. 20–29, October 1955.

[13] T. G. Mihran, "Closed- and open-ridge waveguide," *Proc. IRE*, vol. 37, pp. 640–644, June 1949.